LBL-25747 c.2

Lawrence Berkeley Laboratory
UNIVERSITY OF CALIFORNIA

CHEMICAL BIODYNAMICS DIVISION

LAWRENCE
BERKELEY LABORATORY

DEC 13 1988

LIBRARY AND
DOCUMENTS SECTION

Presented at the C.S. French Symposium, Stanford, CA,
July 18–22, 1988 and to be published
in the Proceedings

Temperature Dependent Steady State and Picosecond Kinetic Fluorescence Measurements of a Photosystem I Preparation from Spinach

I. Mukerji and K. Sauer

August 1988

TWO-WEEK LOAN COPY

This is a Library Circulating Copy
which may be borrowed for two weeks.

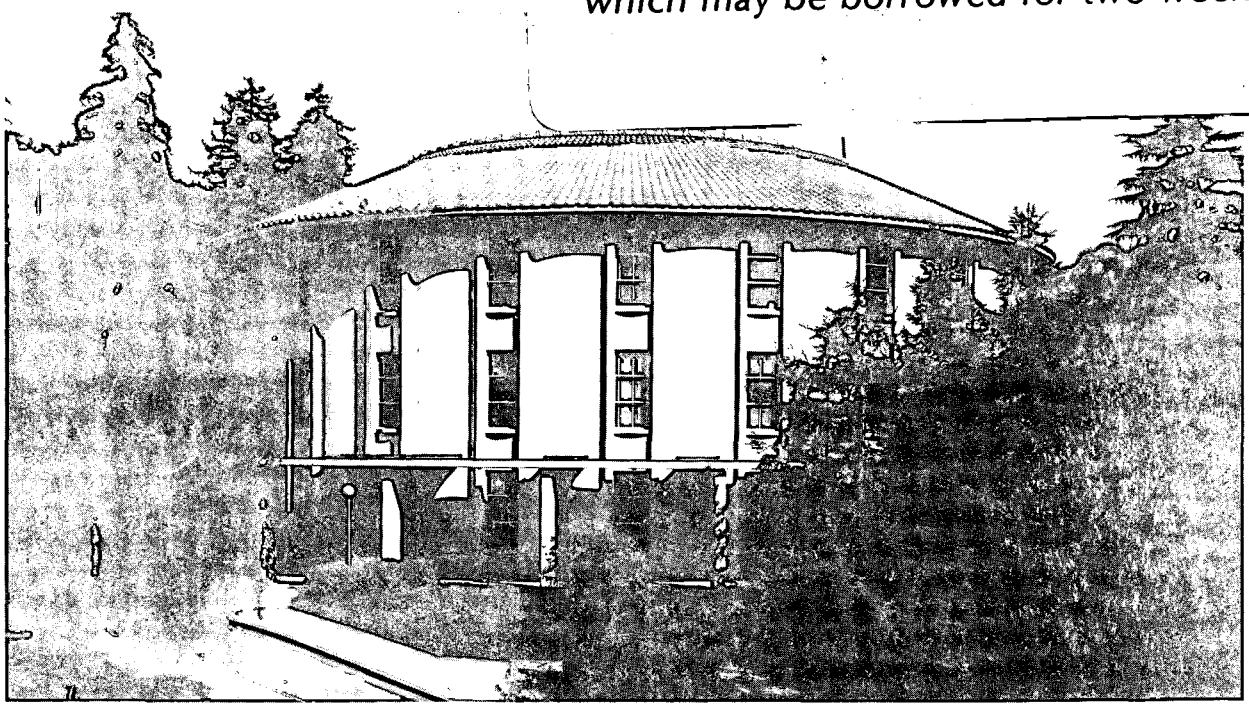

LBL-25747 c.2

Prepared for the U.S. Department of Energy under Contract Number DE-AC03-76SF00098.

DISCLAIMER

This document was prepared as an account of work sponsored by the United States Government. While this document is believed to contain correct information, neither the United States Government nor any agency thereof, nor the Regents of the University of California, nor any of their employees, makes any warranty, express or implied, or assumes any legal responsibility for the accuracy, completeness, or usefulness of any information, apparatus, product, or process disclosed, or represents that its use would not infringe privately owned rights. Reference herein to any specific commercial product, process, or service by its trade name, trademark, manufacturer, or otherwise, does not necessarily constitute or imply its endorsement, recommendation, or favoring by the United States Government or any agency thereof, or the Regents of the University of California. The views and opinions of authors expressed herein do not necessarily state or reflect those of the United States Government or any agency thereof or the Regents of the University of California.

TEMPERATURE DEPENDENT STEADY STATE AND PICOSECOND KINETIC FLUORESCENCE MEASUREMENTS OF A PHOTOSYSTEM I PREPARATION FROM SPINACH

Ishita Mukerji and Kenneth Sauer
Department of Chemistry and Chemical Biodynamics Division
Lawrence Berkeley Laboratory, University of California
Berkeley, Ca 94720 USA

ABSTRACT

The fluorescence properties of a photosystem I (PSI) preparation from spinach containing approximately 200 chlorophyll (Chl) per reaction center were investigated. The preparation, characterized both spectroscopically and biochemically, contained the peripheral light harvesting antenna associated with PSI. In this study steady state fluorescence measurements were performed as a function of temperature. An emission maximum at 690 nm and a long wavelength shoulder from 710 to 740 nm were observed. The fluorescence yield at 690 nm is temperature independent, while the yield of the long wavelength shoulder increases dramatically with decreasing temperature. Additionally, kinetic measurements using the technique of single photon counting were done at room temperature and 77K. At 295K a four component fit was needed to describe the fluorescence decay; whereas at 77K, an additional 40-50 ps rise component indicative of fluorescence induction was necessary. The kinetic measurements demonstrate that the increase in yield as a function of decreasing temperature arises primarily from an increase in fluorescence decay component amplitude rather than an increase in lifetime. The dependence of the yield of the long wavelength emission on excitation wavelength indicates that an integral relationship exists between the chlorophyll b (Chl b) contained in the peripheral light harvesting antenna and the long wavelength emission.

INTRODUCTION

Intact PSI complexes have been isolated with different amounts of core and peripheral antenna pigments associated with the reaction center (Mullet et al.,1980; Lam et al., 1984). A

peripheral light harvesting complex (LHCP-1) containing Chl b is associated with PSI. This light harvesting complex contributes significantly to the long wavelength emission characteristic of PSI at low temperature (Haworth et al., 1983). The core antenna and reaction center are associated with two high molecular mass peptides, approximately 62 and 58 kDa, which bind the primary electron donors and acceptors and 100 Chl a molecules (Fish and Bogorad, 1986; Golbeck et al., 1987; Malkin, 1986). The LHCP-1 complex contains polypeptides in the 20-24 kDa range. This complex consists of 100 Chl a and Chl b molecules in a ratio of approximately 4:1. All of the Chl b in PSI is found in the LHCP-1 complex (Mullet et al., 1980; Lam et al., 1984; Malkin, 1986; Ortiz et al., 1984). In this study the role of Chl b in stimulating long wavelength emission is specifically addressed.

The dynamics of energy transfer between antenna pigments and reaction centers of photosynthetic systems has motivated many spectroscopic studies in recent years (Bose, 1982; Holzwarth, 1987b). The occurrence of uphill energy transfer to the reaction center from a long wavelength absorbing pigment (Butler et al., 1979) causes PSI to be a particularly interesting system for study. Time-resolved emission spectroscopy using the method of single-photon counting is a useful tool for unravelling the mechanisms of energy transfer within photosynthetic systems. Analysis of fluorescence decay kinetics can provide information relating to structure, dynamics of energy transfer and photochemical trapping within a photosynthetic unit. Recently, single-photon counting measurements have led Owens et. al. (1987b) to conclude that a linear relation exists between trapping times and antenna size, indicating that in PSI core preparations excitation migration is trap limited. Although many time-resolved fluorescence studies have been done on chloroplasts at low temperature (Butler et al., 1979; Reisberg et al., 1982; Wittmershaus et al., 1985; Mimuro et al., 1987; Mimuro, 1988; Beddard et al., 1979; Gulotty et al., 1985; Holzwarth et al., 1984) and on PSI reaction-center enriched preparations (Mimuro et al., 1987; Mimuro, 1988; Searle et al., 1988; Owens et al., 1987a; Owens et al., 1988; Wittmershaus, 1987), comparatively few studies have been done on PSI preparations containing more than 100 Chl/reaction center at low temperature (Mimuro et al., 1987; Mimuro, 1988; Wittmershaus, 1987). In this study all measurements were performed on a PSI preparation from spinach containing 200 Chl/P700.

Steady state fluorescence and time resolved emission spectroscopy were done at room temperature and at 77K. Fluorescence decays at 295K were adequately described by 4 components: <30 ps, 80-100 ps, 270-330 ps, and 1.3-1.8 ns. An emission maximum was observed at 690 nm at room temperature with a strong shoulder from 710 to 740 nm. At 77K the emission maximum is red-shifted to 740 nm, and the fluorescence decay kinetics was deconvolved to 5 components: 40-50 ps rise, and decays of 250-280 ps , 1.0-1.1 ns , 2.4-2.5 ns and 4.8-5.3 ns . The fluorescence yield at 740 nm increases about 20 fold with decreasing temperature, arising primarily from an increase in the time-resolved component amplitudes rather than lifetime. Additionally, the ratio of fluorescence yield at 735 nm (F735) to the yield at 690 nm (F690) increases when the excitation is at 650 nm relative to excitation at 670 nm. This effect is observed at both 295K and at 77K. This enhanced yield at longer wavelengths reflects an increase in the amplitude of the 90 ps component at room temperature and the longer lived components at 77K. Steady state measurements confirm the results obtained in the kinetic studies. Because 650 nm is the absorption maximum for Chl b (Clayton, 1986), we conclude that Chl b plays an integral role in stimulating long wavelength emission in PSI.

MATERIALS AND METHODS

The PSI complex (PSI-200) containing the reaction center and a full complement of the antenna was isolated from spinach according to the procedure described by Mullet et. al. (Mullet et al., 1980) with some modifications. All procedures were carried out at 4°C with limited light exposure. Chloroplasts were prepared by grinding market spinach leaves in buffer (0.3M sucrose, 0.01M NaCl, 5.0mM $MgCl_2$ and 50.0mM N-tris[hydroxymethyl]methyl glycine (Tricine), pH=7.8), filtering through 4 layers of cheesecloth, followed by centrifuge spin (1000xg; 5 min). Chloroplasts were resuspended (50.0 mM sorbitol, 0.75mM EDTA, pH=7.8) and then concentrated by centrifugation (11,000xg; 5 min). This step was repeated. Resulting pellets were resuspended (50.0 mM sorbitol, 5.0 mM Tricine, pH=7.8) and then centrifuged (19,000xg; 15 min) to remove soluble components. Pellets were then diluted with ice cold H_2O to a Chl concentration of 0.75-0.8 mg/ml with a Triton-X-100 concentration of 1.0-1.2%

(w/v). These conditions differ depending on the nature of the spinach and the season. This detergent chloroplast mixture was shaken for 1 h at room temperature in a water bath protected from light and then centrifuged (44,000xg; 30 min). The resulting supernatant was immediately loaded onto a 0.1-1.0M linear sucrose density gradient containing 0.02% Triton-X-100 and centrifuged (100,000xg; 16 h). The band of interest occurred at the interface between the 2.0M sucrose cushion and the linear gradient.

Chl concentration and Chl a/b ratios were determined as described by Arnon (1949). Polypeptide composition was determined by SDS-PAGE; separating gels were 12.5% acrylamide and stacking gels were 6.0% acrylamide. Absorption spectra were obtained using a Varian 2300 spectrophotometer in the UV-Vis mode. The amount of Chl per P700 was determined by light-induced absorption changes using an Aminco DW-2 spectrophotometer with side illumination from a tungsten lamp filtered by a Corning 4-96 color filter. Absorption changes were monitored at 699 nm with an EMI GENCOM 9684 (S1 type) photomultiplier tube through a 700 nm narrow bandpass filter using $\Delta\varepsilon=64 mM^{-1}cm^{-1}$ (Hiyama and Ke, 1972). Samples were suspended at 10µg Chl/ ml in 50mM Tris, pH=7.8 and 5mM ascorbate. Steady state fluorescence measurements were performed using a SPEX Fluorolog 2 model 212 spectrofluorimeter with an RCA: C31034A photomultiplier tube. All emission scans were corrected for emission monochromator and photomultiplier tube wavelength dependence. Excitation scans were corrected for lamp and monochromator wavelength dependence. Low temperature fluorescence studies were done using a liquid nitrogen filled cylindrical glass dewar. Samples were diluted to <0.1 absorbance at 675 nm and were frozen to a cracked glass in 60% glycerol, 40% 50.0mM Tricine, pH=7.8 in a glass NMR tube. Variable temperature measurements were done using an Oxford cryostat.

Fluorescence decays were measured by time-correlated single photon counting. Picosecond pulses were provided by a tunable cavity-dumped dye laser (Spectra Physics 375, 341) synchronously pumped by an Ar ion laser (SP 171). DCM was used as the lasing dye. Pulses were issued at a repetition rate of 823 kHz. Emission wavelength was selected by a double monochromator (Instruments, SA) with a 2 nm bandwidth and detected by an ITT microchannel plate detector (model F4129). The instrument response function, measured by scattering the excitation beam with a

solution of non-dairy creamer in H_2O, had a FWHM of 140-150 ps. Deconvolution of the decays with the instrument response function gives a time resolution of 20 ps. Fluorescence decays, following a short flash of exciting light were described in terms of a sum of simultaneous exponential decays

$$F(t)=\Sigma\alpha_i e^{-t/\tau_i}$$

where F is the fluorescence intensity, α_i the amplitude and τ_i the lifetime of the individual components. Quality of the fit was judged by the value of the reduced χ^2 (1.0-1.15) and from a plot of the weighted residuals.

Both single exponential analysis and global analysis (Holzwarth, 1987a) were applied to the decays. When global analysis was used, a set of decays was measured at 5 nm intervals under the same conditions, and the lifetimes were constrained to be constant for the corresponding decay components at all wavelengths. This method of analysis is useful for indicating inadequacies in the model function, as well as for reducing the total number of parameters. It therefore improves the precision and stability of each parameter. The results from the global analysis were consistent with those obtained by analyzing the decays individually with unconstrained lifetimes. Consistency with respect to lifetime and reduced χ^2 values was monitored specifically. The decay component amplitudes at each wavelength obtained from the global analysis were corrected for data collection time, excitation intensity and wavelength dependence of the detector. Decay-associated spectra refer to corrected amplitudes plotted as a function of emission wavelength.

RESULTS

The PSI preparation used for these spectroscopic studies is stable and photochemically active. It contains approximately 200 Chl/ P700 and has a Chl a/b ratio of 8:1. The presence of Chl b is confirmed by prominent shoulders at 472nm and 650nm (Clayton, 1980) in the absorption spectrum (data not shown). SDS-PAGE was used to characterize the polypeptide composition. Reaction center and peripheral antenna polypeptides were observed, as well as low molecular weight polypeptides which possibly bind Fe-S centers (Høj and Moller, 1986). Due to the large antenna complement and the relatively low amounts of

detergents used for isolation, PSI-200 represents a preparation which resembles PSI in vivo (Mullet et al., 1980, Lam et al.,1984).

Fluorescence Temperature Dependence

PSI-200 at room temperature exhibits an emission maximum at 690 nm with a shoulder from 710 to 740 nm; at 77K the emission maximum is red-shifted to 738 nm with a shoulder at 690nm (Mullet et al., 1980; Haworth et al., 1983). In Fig. 1A it can be seen that the intensity of F735 increases approximately 20 fold as a function of decreasing temperature; whereas F690 remains relatively small. Changes in the apparent intensity of F690 result in part from instabilities in the glass at temperatures between 77K and 250K. The maximum of the long-wavelength emission becomes progressively red-shifted as the temperature is decreased (Fig. 1B), which is suggestive that more than one component is contributing to this fluorescence. This temperature dependent fluorescence behavior is not a property of Chl a *in vitro* (Goedheer, 1964). We conclude that for the PSI complex the fluorescence behavior is directly related to changes in excitation quenching and energy transfer dynamics. Additionally, the relative fluorescence intensity of the long wavelength shoulder is dependent on excitation wavelength. At 295K excitation was done at 435, 472, 650 and 670 nm. The highest fluorescence yield was observed with excitation at 435 nm. Excitation spectra confirm that Chl b particularly sensitizes long wavelength emission at both 295K and 77K. (Fig. 2A) Excitation at the Chl b absorption maxima enhances the relative fluorescence yield of the long wavelength shoulder with respect to emission at 690nm. When excitation is at 472nm, there is an unknown amount of contribution from carotenoid absorption;however, carotenoids do not contribute to the absorption at 650 nm (Fig. 2B). This enhanced yield was observed also at 77K (data not shown).

Picosecond Fluorescence Kinetics

The time resolved fluorescence decay measurements on PSI-200 excited at 650nm or 670nm at 295K were fit to a sum of four exponentials (Fig. 3). Although Owens et. al. (1988) report decays which fit to 3 components for smaller PSI complexes, we find that the PSI-200 complex with an extended antenna requires an additional component.

Our data were taken over the emission wavelength range 685-740nm. The data obtained were analyzed globally using both a 3-exponential and a 4-exponential model. The weighted residuals of the fits are shown in Fig. 4A and 4B. It is apparent from the plot of the weighted residuals and a comparison of the χ^2 values that the 4-exponential model best satisfies the data at room temperature.

In contrast to Owens et. al. (1988) we find that the lifetime of the shortest decay component is relatively independent of emission wavelength, regardless of excitation at 650 nm or at 675 nm. The single wavelength analysis lifetimes are independent of emission wavelength within the experimental uncertainty (± 10%) and are in good agreement with the lifetimes obtained from global analysis (see Table I).

Fluorescence yields for λ_{ex}=675 nm, generated from global analysis, are plotted vs. wavelength in Fig. 5A. The fluorescence yield of each component is defined as:

$$\phi_i = \alpha_i \tau_i$$

The <30 ps component constitutes approximately 90% of the amplitude, corresponding to 70% of the fluorescence yield at its emission maximum at 695 nm. This component, although at the limit of our time resolution, dominates the decay profile owing to its large amplitude. The 80-100 ps component contributes approximately 60% of the overall yield at its emission maximum at 730nm. The corrected yield arising from the middle component, 270-330 ps, is relatively wavelength independent and contributes 10% to the yield. The slowest component, 1.3-1.8 ns appears to have an emission maximum wavelength shorter than 685nm and adds at most 4% to the total fluorescence yield.

Fig. 5B depicts a decay associated spectrum from global analysis, where λ_{ex}=650 nm. The ratio of the fluorescence yields ϕ730/ϕ690 for the 80-100 ps component increases when excitation is at 650nm relative to that for excitation at 670 nm. This enhancement of the long wavelength fluorescence through Chl b excitation is seen in both the kinetic measurements and the steady state measurements. Our data are suggestive that Chl b particularly sensitizes long wavelength emission, reflected by the increase in relative yield of the 80-100 ps decay component.

Fig. 6A shows a decay associated spectrum of PSI-200 at 77K with λ_{ex}=670nm. The decays were analyzed by global analysis using a 5 component model. From global analysis it was determined that

a 4 exponential model was not sufficient to describe the data. The lifetime of each of the components is 2-3 times longer than those observed at room temperature. In the slower components the dominant effect of lowering the temperature appears to be an increase in amplitude, whereas in the faster components the amplitudes are relatively unaffected.

The fastest component, 50 ps, comprises about 95% of the amplitude at 695nm. This component also exhibits a negative amplitude, indicative of fluorescence induction, at wavelengths >720nm. The maximum of the negative amplitude occurs at 735nm. Additionally, a fast decay of 250-280 ps is observed which has an emission maximum at 720nm and contributes 55% of the amplitude at that wavelength. The slowest decay component, 4.8-5.3 ns, has an emission maximum at wavelengths <680 nm and contributes at most 3% to the overall amplitude. The 1.0-1.1 ns component has a broad maximum at 725-730nm and contributes about 40% to the total amplitude. The 2.4-2.5 ns decay peaks at 750nm, comprising approximately 70% of the total amplitude. It is apparent from the decay associated spectra (Figs. 6A and 6B) that excitation at 650nm increases the amplitudes of the slower decay components (0.25 ns, 1.1 ns, 2.4 ns) at longer wavelengths relative to the amplitude of the fast decay at 695nm.

DISCUSSION

Mimuro et. al. have made time-resolved spectroscopic measurements on PSI complexes similar in antenna size and isolation procedure to the PSI-200 preparation (Mimuro et al., 1987; Mimuro, 1988). The lifetimes obtained in the present work agree with the 4 components they used to deconvolute room temperature data (Mimuro et al., 1987). Measurements at 77K (Mimuro, 1988) were deconvoluted to 7 components, including three designated F720, F735 and F747. The emission peaks of the slower decay components obtained in our study correlate with the 3 longest wavelength components identified by Mimuro.

Wittmershaus (1987) reports lifetimes of 11 ps and 89 ps for PSI particles using a streak camera to observe room temperature emission at 685nm; at 77K lifetimes of 12 ps and 305 ps are reported. Their data were fit to only 2 exponential decay components. The effect of temperature on the amplitudes of these components

was not addressed.

Our results confirm and extend those that have been previously reported. The lifetimes presented in this study correlate well with those of Mimuro and Wittmershaus. Additionally, our results support the biochemical data (Mullet et al., 1980; Haworth et al., 1983) which are suggestive that the longest wavelength emission in PSI arises primarily from the peripheral light harvesting antenna. We have observed both at 295K and at 77K that excitation at the absorption maxima of Chl b enhances fluorescence at 735 nm. As Chl b is found only in LHCP-1 in PSI, this complex appears to be directly connected to the longest wavelength emission observed at both RT and 77K. This previously unreported result has been confirmed by both steady state and time-resolved emission studies.

Additionally, we observe from kinetic measurements at 77K that the exponential decay component amplitudes are the dominant factor for the dramatic increase in yield. We believe that the increase in amplitude reflects an increase in photon capture cross-section, caused by a decrease in the rate of photochemical trapping at lower temperatures. The fluorescence decay lifetimes increase by a factor of 3; however, the yield increases by approximately 20 fold between 290 and 80K. The majority of the fluorescence yield increase appears to arise from the increased amplitudes of the two longer lived decay components which peak at 730nm and 740nm. (Fig. 7) Studies of the temperature dependence of a PSI complex (CPI) with a smaller antenna indicated that, in that case also, the increased yield arises primarily from an increase in amplitude of the individual decay components (Tabbutt, 1987).

We propose that the kinetic component 1, (F690, see Table I) arises from the core antenna, while component 2 (F720) stems from an internal antenna. At 295K Chl b excitation increases the yield of this component, implying that the peripheral light harvesting antenna transfers energy to this antenna complex. Excitation transfer from F735 to F720 is not resolved in our measurements, as we observe no rise time. We assign the slowest decay component to dissociated Chl or to antenna which lack a functional trap. Such slowly decaying fluorescence amounts to no more that 3% of the total amplitude. We attribute kinetic components 3 (F735) and 4 at 77K to the peripheral light harvesting antenna.

We suggest a model (Fig. 8) for energy transfer within PSI, which attempts to explain both

the increase in lifetime and amplitude at lower temperatures. Searle et. al. (1988) have proposed a model for a smaller antenna system; we have modified and extended this model to encompass the system used in this study. Our model consists of 3 distinct antenna forms: F690, F720 and F735 and a photochemical trap, P700. We propose that the efficiency of the trapping reaction $P700 \rightarrow P700^{+}$ decreases with decreasing temperature. Additionally, excitation transfer from F735 to F720 and from F720 to P700 are both endothermic and temperature dependent. Fluorescence is a decay path for excited F720 and F735. We assume that most of the excitation arises from absorption by the main antenna Chl molecules and visits the reaction center before reaching F720 or F735. Excited F690 decays by temperature independent transfer to P700 or by fluorescence. The increase in lifetime at lower temperatures reflects the decrease in rate constant for the trapping reaction. Consequently, excitation visiting P700, which would normally be trapped, is now diverted to F720 and F735, increasing the effective photon-capture cross-section of these two components. The increased cross-section results in the increase in amplitude of the corresponding components observed in the time-resolved fluorescence relaxation. Other de-excitation paths such as triplet formation and internal conversion to the ground state exist for P700*; however, the effect of temperature on the yield of these reactions with respect to the fluorescence yield has not been reported. Further experiments need to be done to verify that the trapping reaction is indeed temperature dependent. A detailed analysis of this kinetic model will appear later.

ACKNOWLEDGEMENTS

We would like to thank Dr. Alfred Holzwarth of the Max Planck Institute of Radiation Chemistry, Mülheim/Ruhr for generously supplying the data analysis programs. This research was supported by the Director, Office of Basic Energy Services, Division of Biological Energy Research of the Department of Energy under contract DE-AC03-76SF00098.

REFERENCES

Arnon DI (1949). Copper enzymes in isolated chloroplasts. Polyphenoloxidase in *Beta vulgaris*. Plant Physiol 24:1-15.

Beddard GS, Fleming GR, Porter G, Searle GFW, Synowiec JA (1979). The fluorescence decay kinetics of *in vivo* chlorophyll measured using low intensity excitation. Biochim Biophys Acta 545:165-174.

Bose S (1982). Chlorophyll fluorescence in green plants and energy transfer pathways in photosynthesis. Photochem. Photobiol. 36:725-731.

Butler WL, Tredwell CJ, Malkin R, Barber J (1979). The relationship between the lifetime and yield of the 735 nm fluorescence of chloroplasts at low temperature. Biochim Biophys Acta 545:309-315.

Clayton RK (1980). "Photosynthesis: Physical mechanisms and Chemical Patterns." Cambridge: Cambridge University Press, p.38.

Fish LE, Bogorad L (1986). Identification and analysis of the maize P700 chlorophyll a apoproteins PSI-A1 and PSI-A2 by high pressure liquid chromatography analysis and partial sequence determination. J Biol Chem 261:8134-8139.

Goedheer JC (1964). Fluorescence bands and chlorophyll a forms. Biochim Biophys Acta 88:304-317.

Golbeck JH, Parrett KG, McDermott AE (1987). Photosystem I charge separation in the absence of centers A and B. III. Biochemical characterization of a reaction center particle containing P700 and F_X. Biochim Biophys Acta 893:149-160.

Gulotty RJ, Mets L, Alberte RS, Fleming GR (1985). Picosecond fluorescence study of photosynthetic mutants of *Chlamydomonas reinhardii*: Origin of the fluorescence decay kinetics of chloroplasts. Photochem Photobiol 41:487-496.

Haworth P, Watson JL, Arntzen CJ (1983). The Detection, isolation and characterization of a light-harvesting complex which is specifically associated with photosystem I. Biochim Biophys Acta 724:151-158.

Hiyama T, Ke B (1972). Difference spectra and extinction coefficients of P700. Biochim Biophys Acta 267:160-171.

Holzwarth AR (1987a). A Model for the functional antenna organization and energy distribution in the photosynthetic apparatus of higher plants and green algae. In Biggins J (ed): "Progress in Photosynthesis Research," Vol. I, The Hague: Martinus Nijhoff, pp 53-60.

Holzwarth AR (1987b). Picosecond fluorescence spectroscopy and energy transfer in photosynthetic antenna pigments. In Barber J

(ed): "The Light Reactions," Amsterdam: Elsevier, pp 95-157.
Holzwarth AR, Haehnel W, Wendler J, Suter G, Ratajczak R (1984). Picosecond fluorescence kinetics and energy transfer in antennae chlorophylls of green algae and membrane fractions of thylakoids. In Sybesma C (ed): "Advances in Photosynthesis Research," Vol I, The Hague: Martinus Nijhoff, pp 73-76.
Høj PB, Moller BL (1986). The 110 kDa reaction center protein of photosystem I, P700-chlorophyll a-protein 1, is an iron-sulfur protein. J Biol Chem 261:14292-14300.
Lam E, Ortiz W, Malkin R (1984). Chlorophyll a/b proteins of photosystem I. FEBS Lett 168:10-14.
Malkin R (1986). A consideration of the organization of chloroplast photosystem I. Photosynthesis Res. 10:197-201.
Mimuro M (1988). Analysis of excitation energy transfer in thylakoid membranes by the time-resolved fluorescence spectra. In Scheer H, Schneider S (eds): "Photosynthetic Light Harvesting Systems," Berlin: W. de Gruyter, pp 589-600.
Mimuro M, Yamazaki I, Tamai N, Yamazaki T, Fujita Y (1987). Analysis of the excitation energy transfer in spinach chloroplasts at room temperature: Identification of the component bands by the time-resolved fluorescence spectrum and by convolution of the decay kinetics. In Kobayashi T (ed): "Primary Processes in Photobiology," Berlin: Springer, pp 23-32.
Mullet JE, Burke JJ, Arntzen CJ (1980). Chlorophyll proteins of photosystem I. Plant Physiol 65:814-822.
Ortiz W, Lam E, Ghirardi M, Malkin R (1984). Antenna function of a chlorophyll a/b protein complex of photosystem I. Biochim Biophys Acta 766:505-509.
Owens TG, Webb SP, Alberte RS, Mets L, Fleming GR (1988). Antenna structure and excitation dynamics in photosystem I. I. Studies of detergent-isolated photosystem I preparations using time-resolved fluorescence analysis. Biophys. J. 53:733-745.
Owens TG, Webb SP, Eads DD, Alberte RS, Mets L, Fleming GR (1987a). Time-resolved fluorescence decay kinetics in photosystem I. Experimental estimates of charge separation and energy transfer rates. In Biggins J (ed): "Progress in Photosynthesis Research," Vol I, The Hague: Martinus Nijhoff, pp 83-86.
Owens TG, Webb SP, Mets L, Alberte RS, Fleming GR (1987b). Antenna size dependence of fluorescence

decay in the core antenna of photosystem I: Estimates of charge separation and energy transfer rates. Proc Natl Acad Sci USA 84:1532-1536.

Reisberg P, Nairn JA, Sauer K (1982). Picosecond fluorescence kinetics in spinach chloroplasts at low temperature. Photochem Photobiol 36:657-661.

Searle GFW, Tamkivi R, van Hoek A, Schaafsma TJ (1988). Temperature dependence of antennae chlorophyll fluorescence kinetics in photosystem I reaction centre protein. J Chem Soc, Faraday Trans 2 84:315-327.

Tabbutt S (1987). Temperature dependence of CPI fluorescence. In "Spectroscopic Studies of Energy Transfer in Photosynthetic Reaction Centers of Higher Plants," PhD. Thesis Berkeley: Lawrence Berkeley Laboratory Report (LBL-24017) pp 105-165.

Wittmershaus B (1987). Measurements and kinetic modeling of picosecond time-resolved fluorescence from photosystem I and chloroplasts. In Biggins J (ed): "Progress in Photosynthesis Research," Vol. I, The Hague: Martinus Nijhoff, pp. 75-82.

Wittmershaus B, Nordlund TM, Knox WH, Knox RS, Geacintov NE, Breton J (1985). Picosecond studies at 77K of energy transfer in chloroplasts at low and high excitation intensities. Biochim Biophys Acta 806:93-106.

FIGURE CAPTIONS

Fig.1. Temperature dependence of PSI-200 fluorescence

A) Steady state fluorescence emission spectra of PSI-200 at 77K, 123K, 169K, 224K, 273K, 292K. Samples originally in 1 M sucrose were diluted 5 fold in 40% 50.0mM Tricine, pH=7.8, 60% glycerol. Excitation was at 435 nm. All spectra were taken on the same sample.

B) Steady state fluorescence measurements of PSI-200 at 77K, 113K, 143K, 167K, 222K, 246K. Sample preparation is the same as in Fig.1A. Excitation done at 435nm on different samples. Spectra are normalized at their emission maxima.

Fig.2. PSI-200 Fluorescence dependence on excitation wavelength

A) Steady state excitation spectra at 77K with emission at 690 nm or 740 nm. Samples frozen to a cracked glass in 60% glycerol/40% 50.0mM Tricine, pH=7.8.

B) Steady state emission spectra at 295K, normalized to emission maxima. Excitation at 435 nm, 472 nm, 650 nm or 670 nm. Samples diluted 5-10 fold in 50.0 mM Tricine, pH=7.8 from 1M sucrose.

Fig.3. Fluorescence decay of PSI-200 at room temperature. Below: Measured fluorescence decay with calculated fit and instrument response function. Above: Weighted residuals. Decay deconvolved to four components. Sample diluted in 50.0mM Tricine, pH=7.8, to 10μgChl/ml. λ_{ex}=670nm. λ_{em}=690nm.

Fig.4. Weighted residuals from global analysis of a set of decays measured on PSI-200. λ_{ex}=670nm. Emission range from 685nm to 735nm. Sample preparation as in Fig.3.

A) Residuals from 3 exponential model. χ^2=1.40.

B) Residuals from 4 exponential model. χ^2=1.16. Scale decreased by a factor of 2 relative to Fig. 4A.

Fig.5. Decay associated spectra of the components determined by a 4-exponential global analysis. Data were taken at 295K. Fluorescence yield of each component is plotted as a function of emission wavelength.

A) λ_{ex}=675 nm.

B) λ_{ex}=650 nm.

Fig.6. Decay associated spectra determined from a 5 componentglobal analysis. Data were taken at 77K. The amplitude of each component is plotted as a function of emission wavelength.

A) λ_{ex}=670nm.

B) λ_{ex}=650nm.

Fig.7. Decay associated spectra of the components determined by a 5-exponential global analysis at 77K. The fluorescence yield of each component is plotted as a function of emission wavelength. λ_{ex}=670nm.

Fig.8. Proposed model of antenna organization and excitation transfer dynamics in PSI-200.

TABLE I

Decay-Associated Spectra obtained from Global Analysis of Fluorescence Kinetics from PSI-200

Kinetic components	1	2	3	4	5
Temperature=295K					
Global analysis lifetimes (ns)	0.018[a] ±0.010	0.085[b] ±0.010	0.30 ±0.04	1.53 ±0.19	
Emission maximum (nm)	695	730	-	<685	
Temperature=77K					
Global analysis lifetimes (ns)	0.045[c] ±0.005	0.27 ±0.02	1.05 ±0.07	2.48 ±0.06	4.99 ±0.21
Emission maximum (nm)	695 (pos. amp.) 735 (neg. amp.)	720	725-730 (broad)	750	<680

Average lifetimes obtained from single wavelength analyses:
[a]0.024 ns
[b]0.102 ns
[c]0.049 ns

Figure 1A

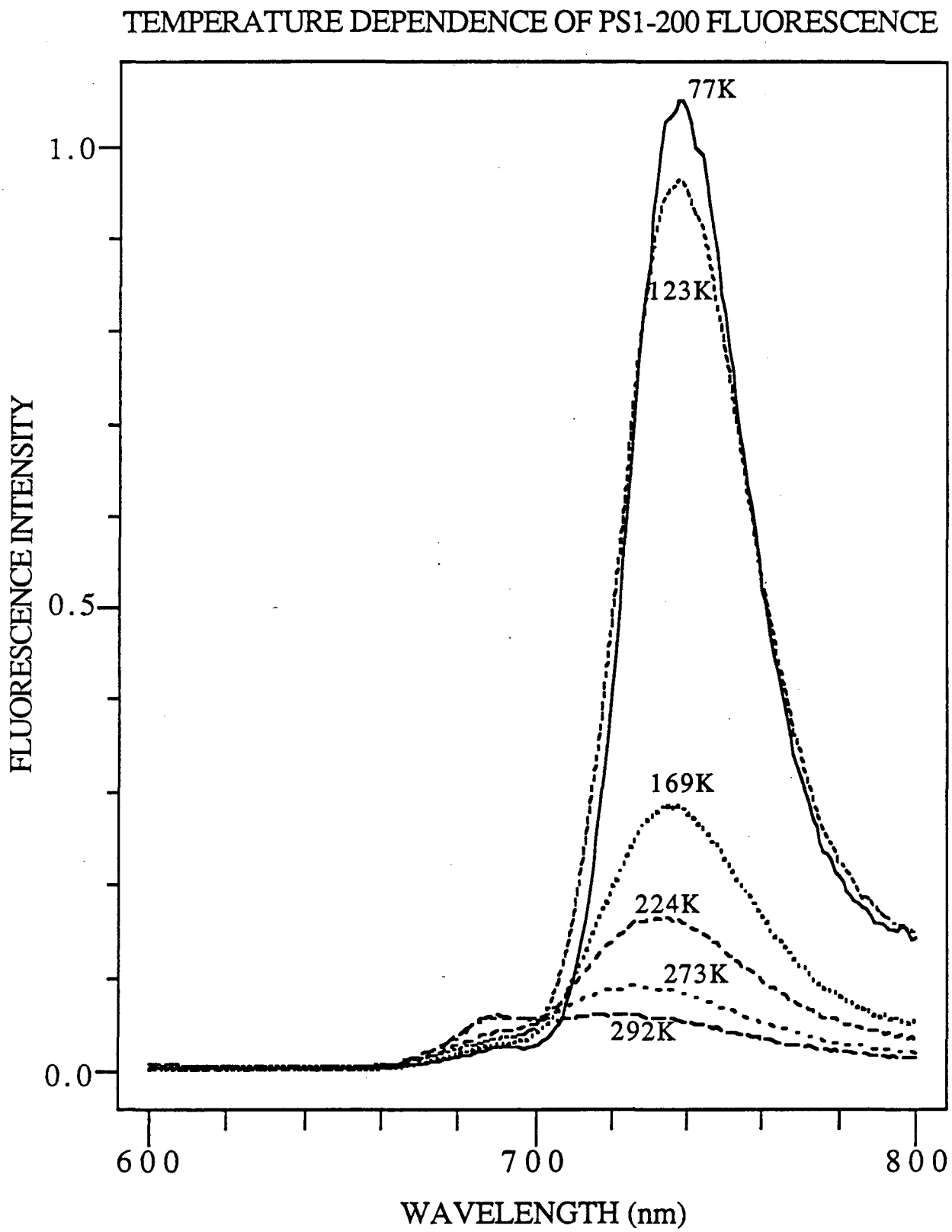
TEMPERATURE DEPENDENCE OF PS1-200 FLUORESCENCE
77K
123K
169K
224K
273K
292K
1.0
0.5
0.0
FLUORESCENCE INTENSITY
600
700
800
WAVELENGTH (nm)

Figure 1B

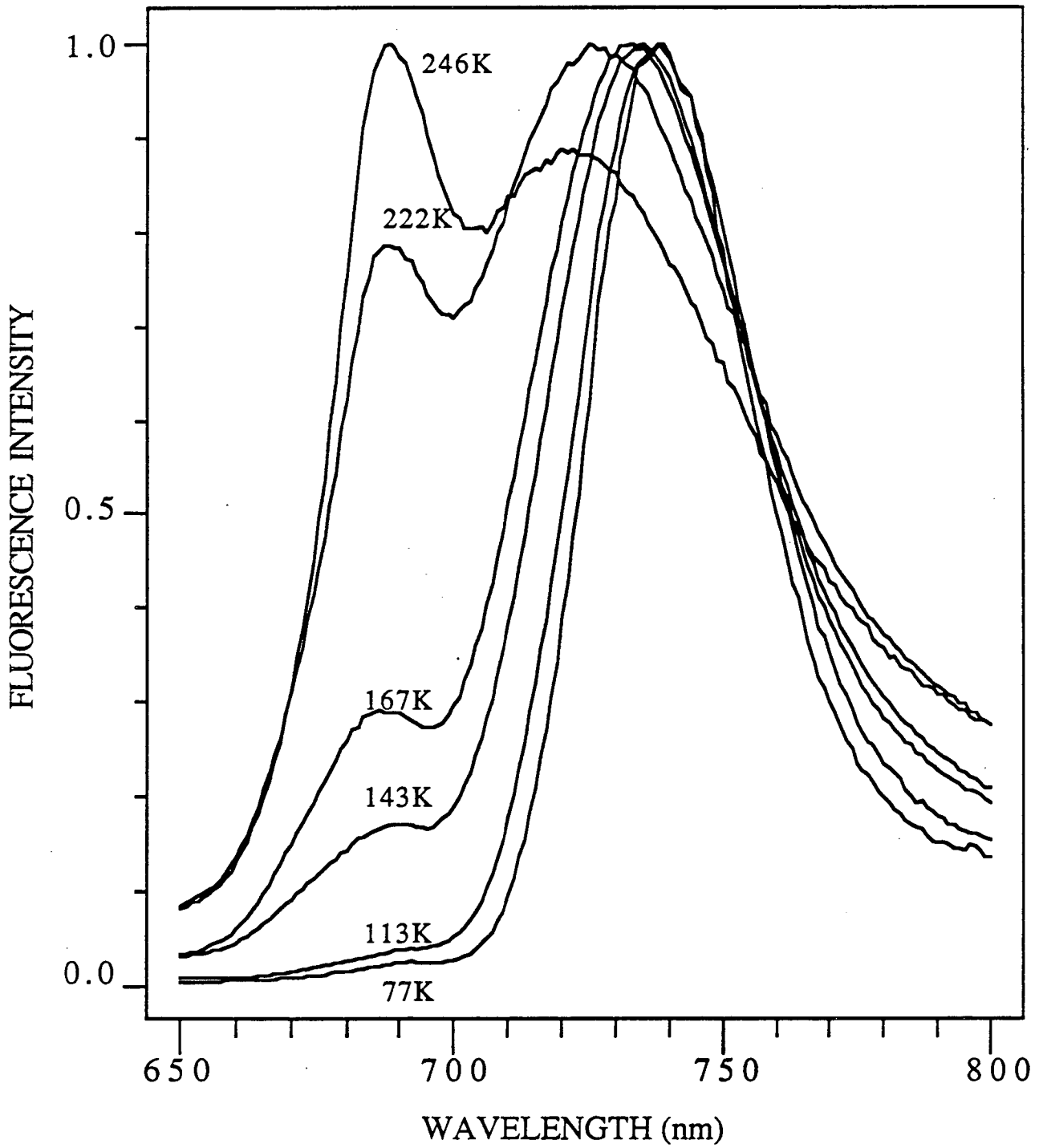
1.0
0.5
0.0
FLUORESCENCE INTENSITY
246K
222K
167K
143K
113K
77K
650
700
750
800
WAVELENGTH (nm)

Figure 2A

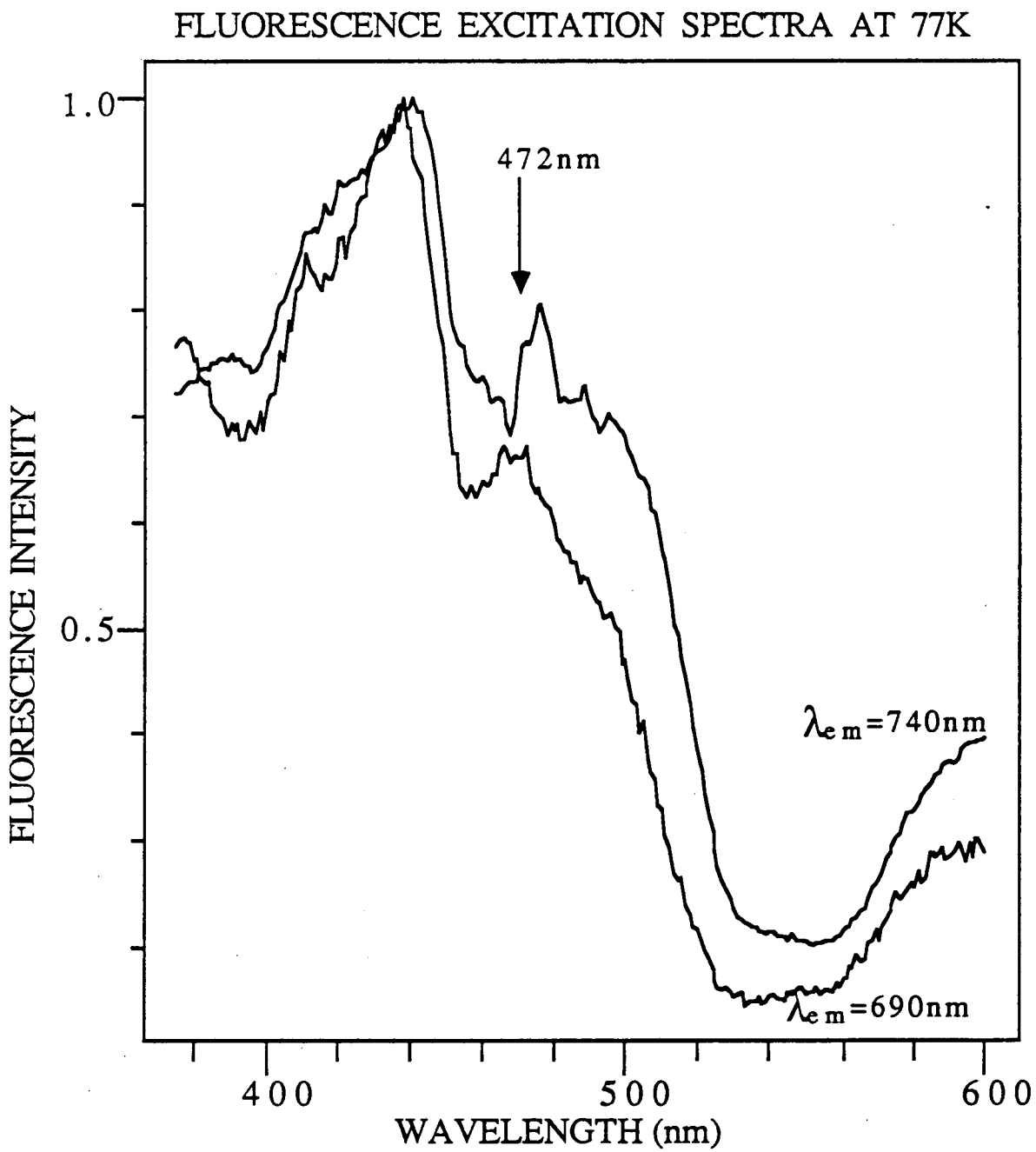
FLUORESCENCE EXCITATION SPECTRA AT 77K
1.0
0.5
FLUORESCENCE INTENSITY
472nm
λem=740nm
λem=690nm
400
500
600
WAVELENGTH (nm)

Figure 2B

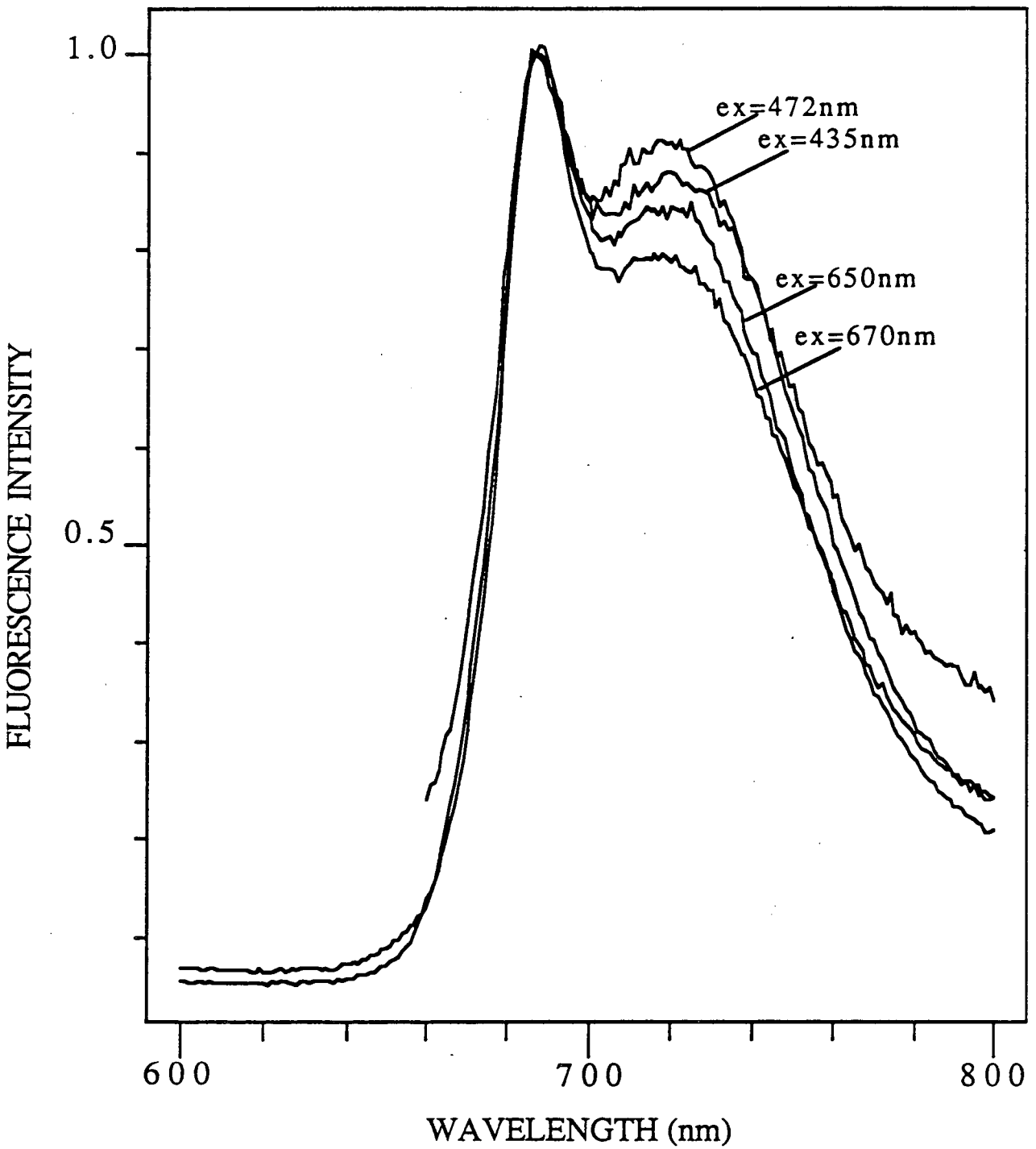
1.0
0.5
FLUORESCENCE INTENSITY
ex=472nm
ex=435nm
ex=650nm
ex=670nm
600
700
800
WAVELENGTH (nm)

Figure 3

λ_{ex}=670nm λ_{em}=690nm

χ^2 =1.007 SHIFT: 0.075

τ(ns):	0.029	0.090	1.860	0.327
α_i:	30.81	5.711	0.022	0.412

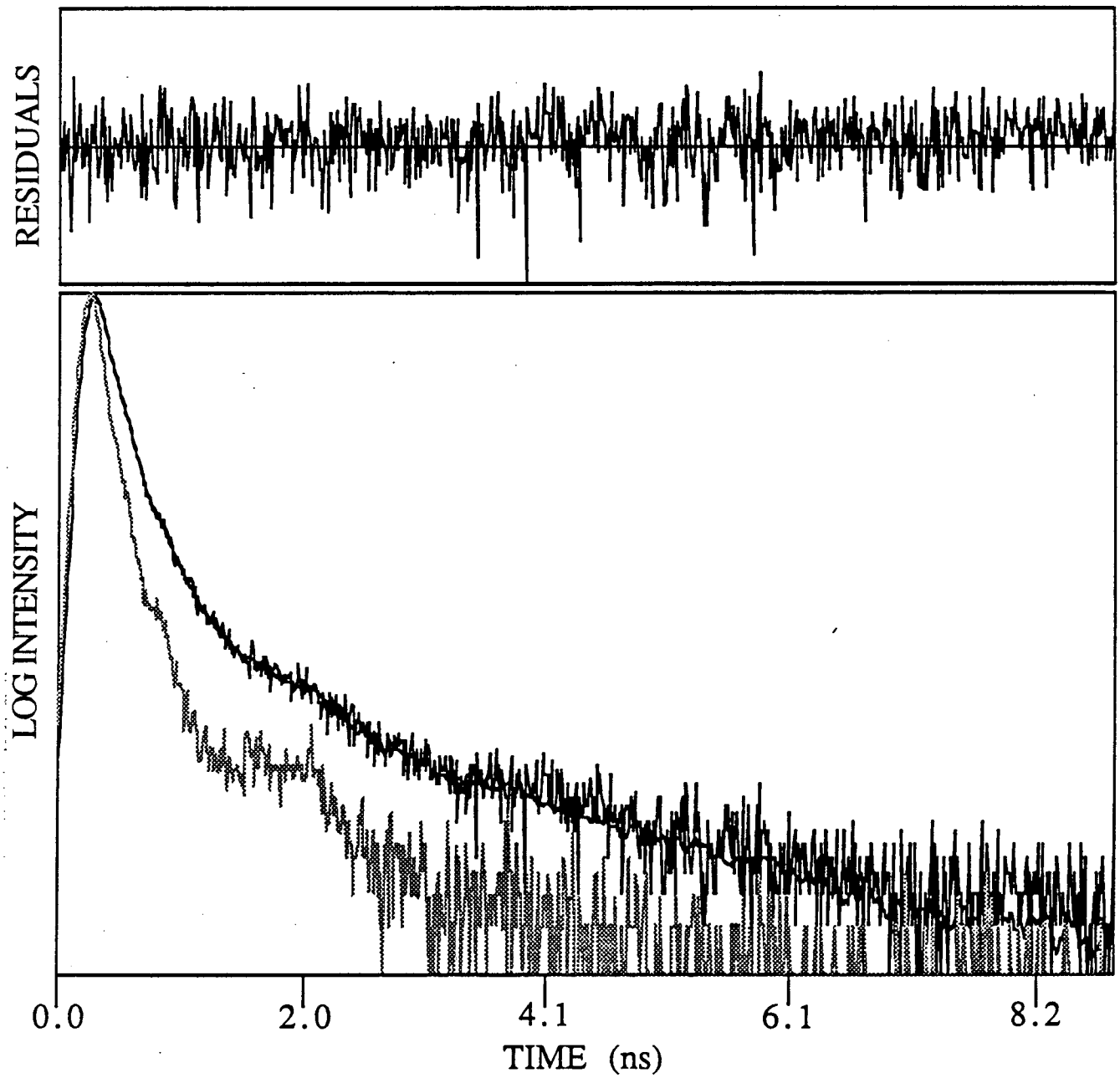

Figure 4A

Residuals from Global Analysis: 3 components

$\chi^2 = 1.4052$

$\lambda_{ex} = 670nm$

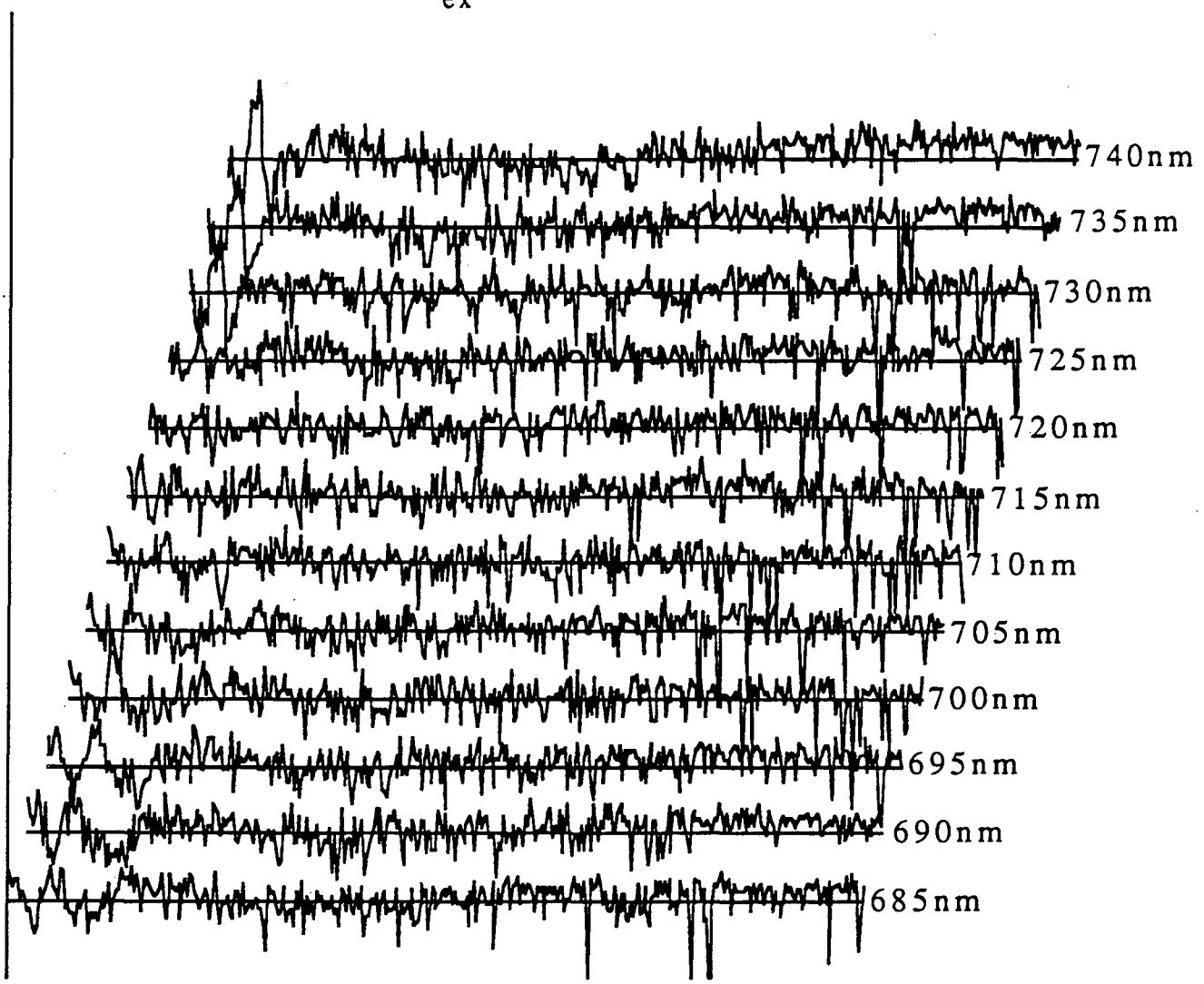

Figure 4B

Residuals from Global analysis: 4 components

$\chi^2=1.1649$

$\lambda_{ex}=670nm$

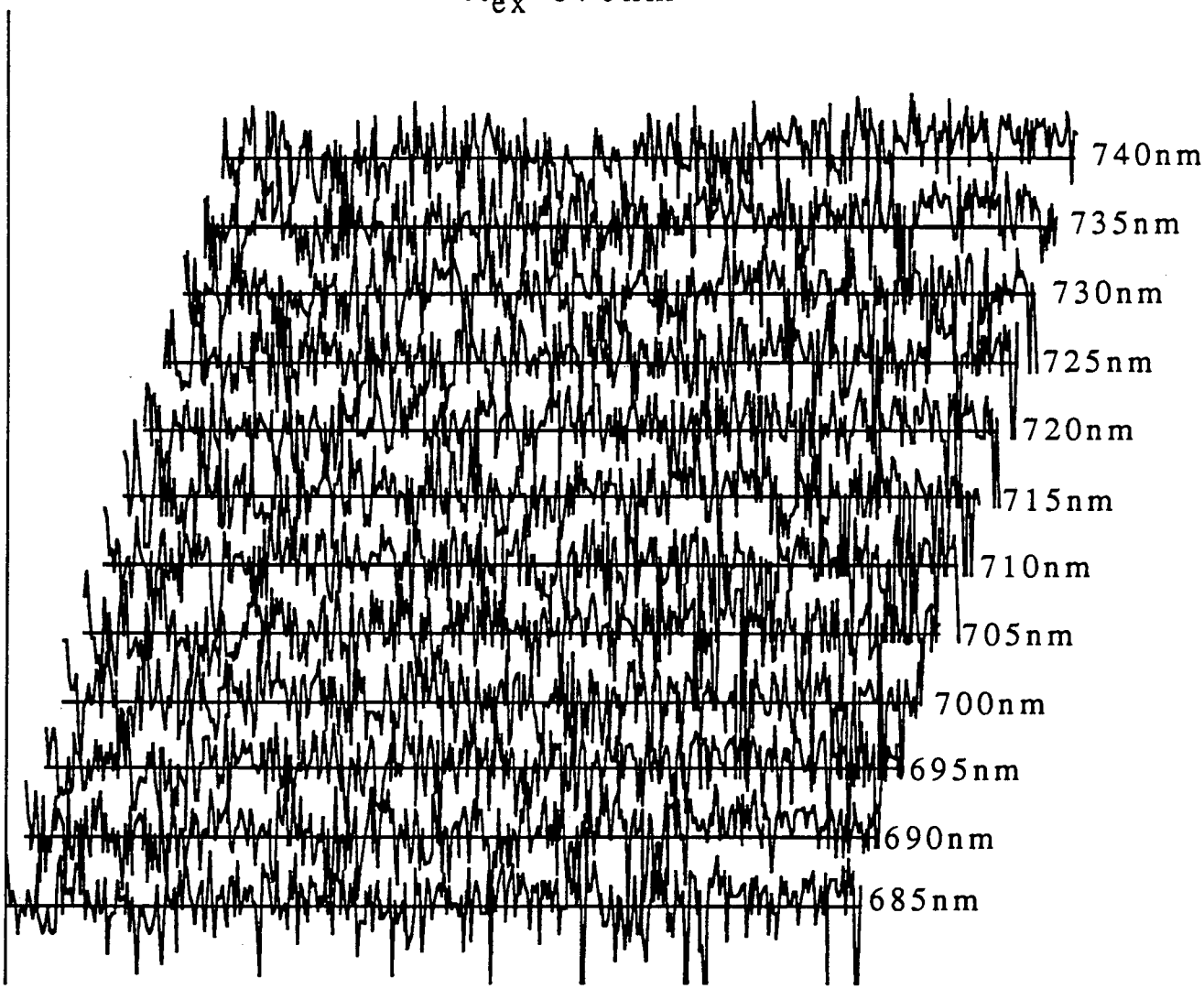

Figure 5A

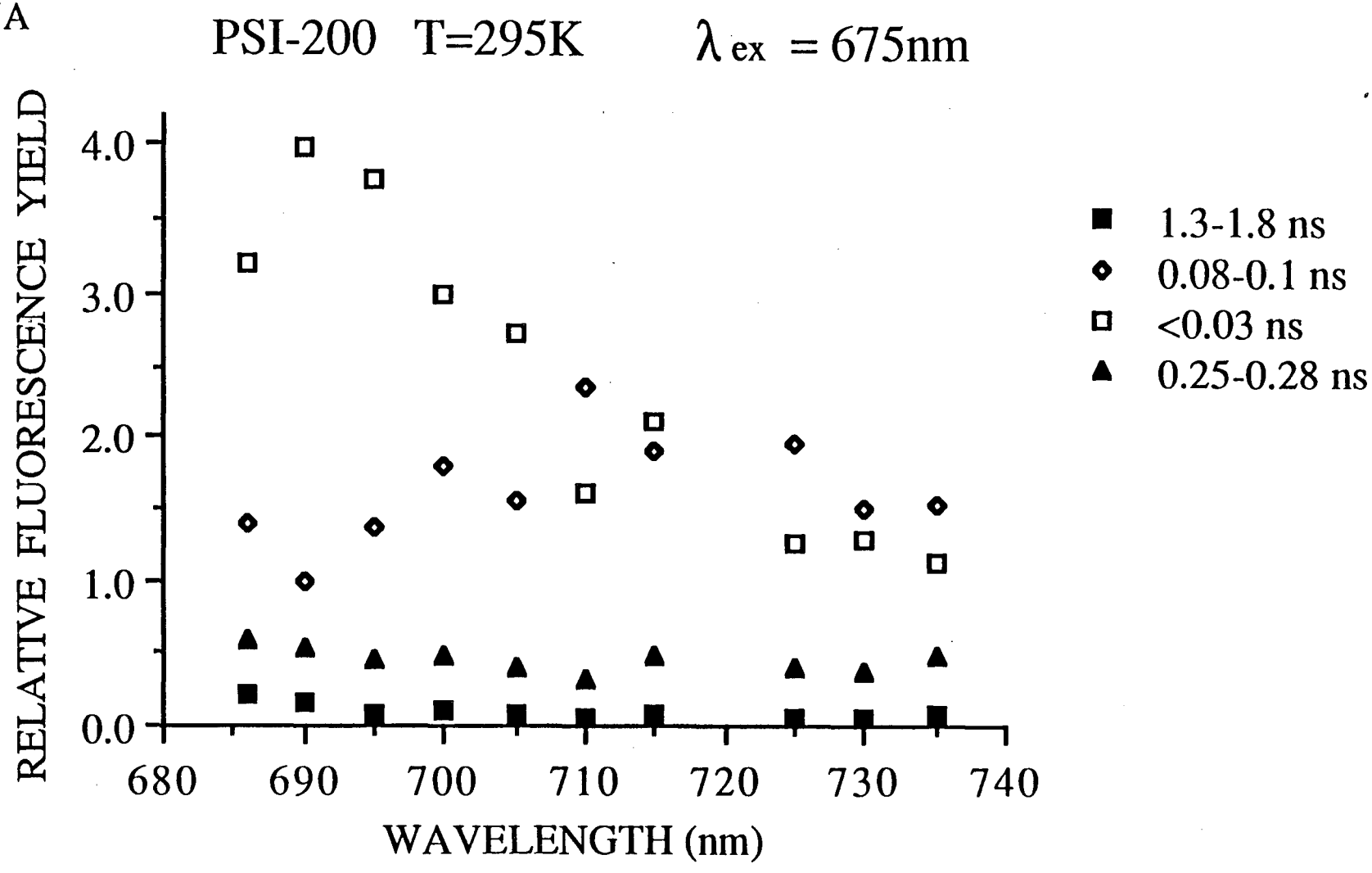
PSI-200 T=295K
λ ex = 675nm
RELATIVE FLUORESCENCE YIELD
4.0
3.0
2.0
1.0
0.0
680
690
700
710
720
730
740
WAVELENGTH (nm)
1.3-1.8 ns
0.08-0.1 ns
<0.03 ns
0.25-0.28 ns

Figure 5B

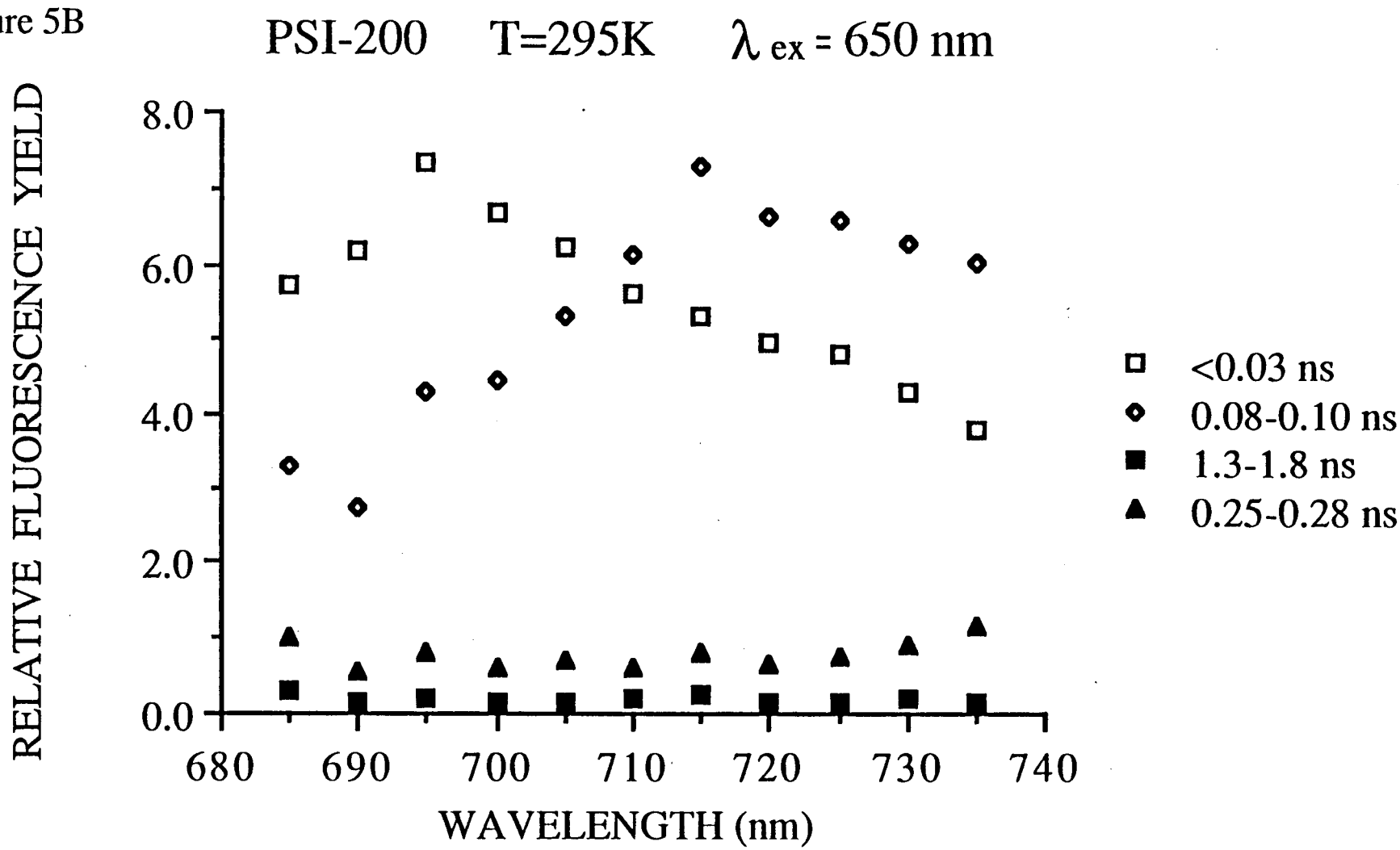
PSI-200 T=295K λ ex = 650 nm
RELATIVE FLUORESCENCE YIELD
8.0
6.0
4.0
2.0
0.0
680
690
700
710
720
730
740
WAVELENGTH (nm)
<0.03 ns
0.08-0.10 ns
1.3-1.8 ns
0.25-0.28 ns

Figure 6A

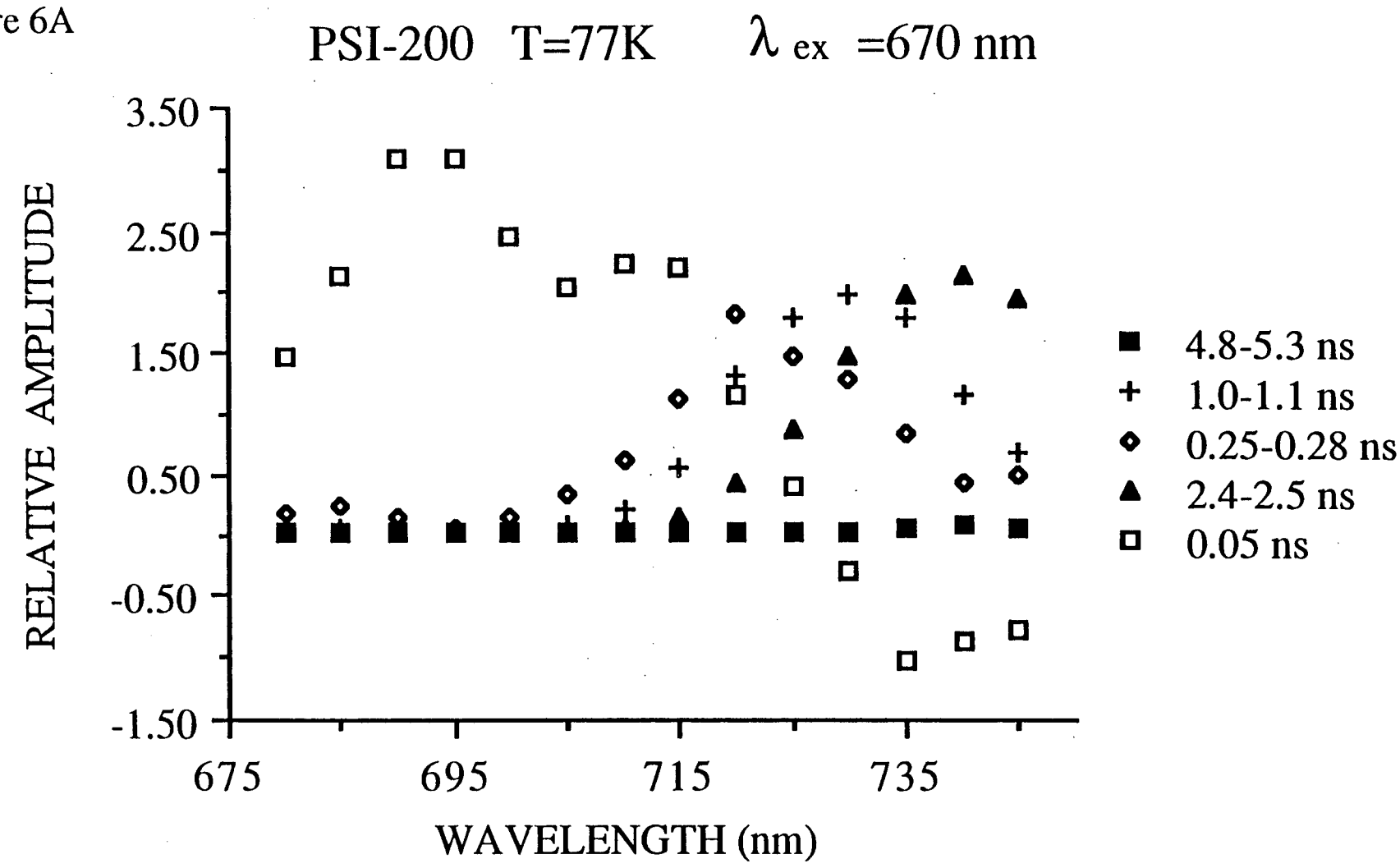
PSI-200 T=77K λ ex =670 nm
RELATIVE AMPLITUDE
3.50
2.50
1.50
0.50
-0.50
-1.50
675
695
715
735
WAVELENGTH (nm)
4.8-5.3 ns
1.0-1.1 ns
0.25-0.28 ns
2.4-2.5 ns
0.05 ns

Figure 6B

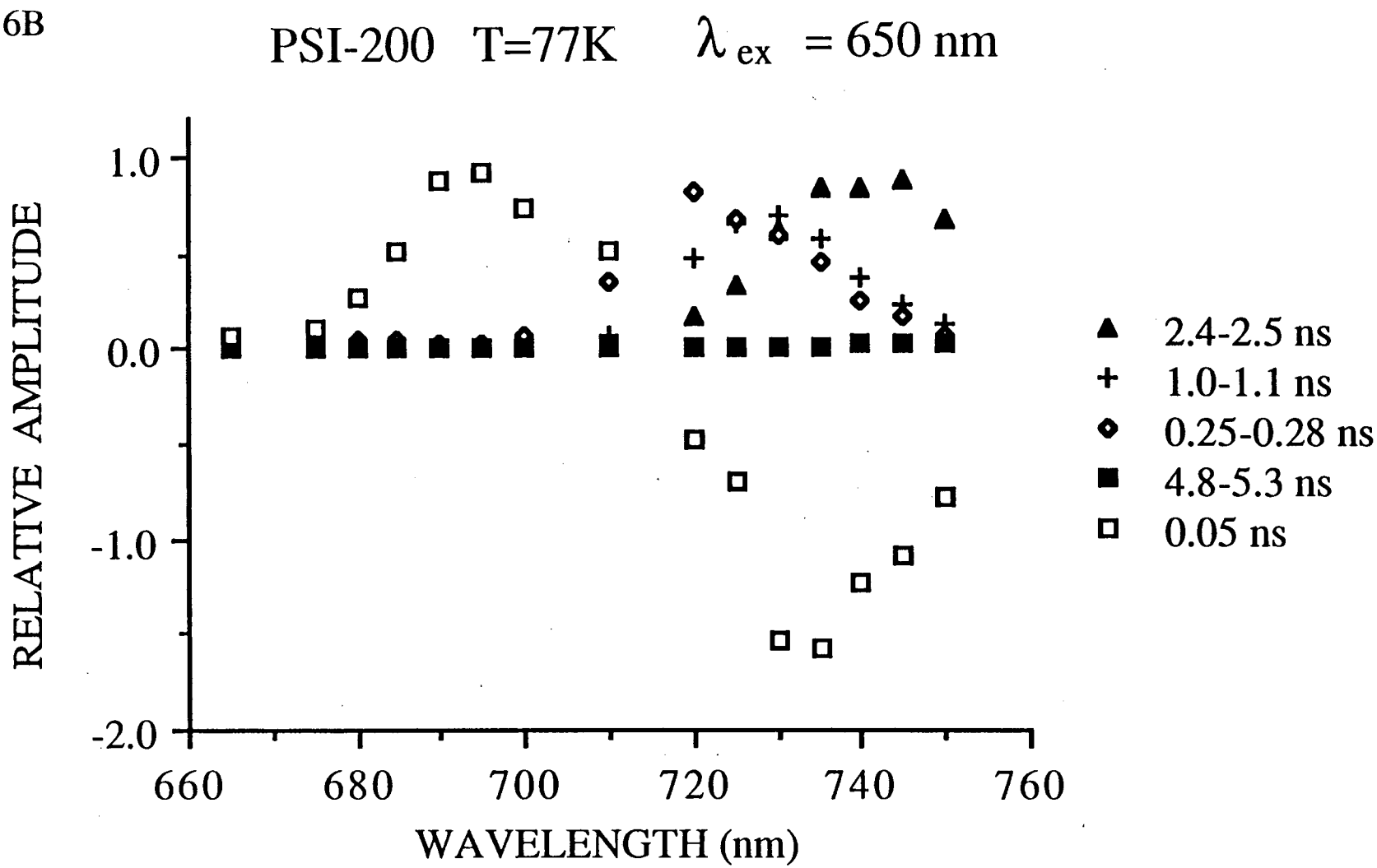
PSI-200 T=77K λ ex = 650 nm
RELATIVE AMPLITUDE
1.0
0.0
-1.0
-2.0
660
680
700
720
740
760
WAVELENGTH (nm)
2.4-2.5 ns
1.0-1.1 ns
0.25-0.28 ns
4.8-5.3 ns
0.05 ns

Figure 7

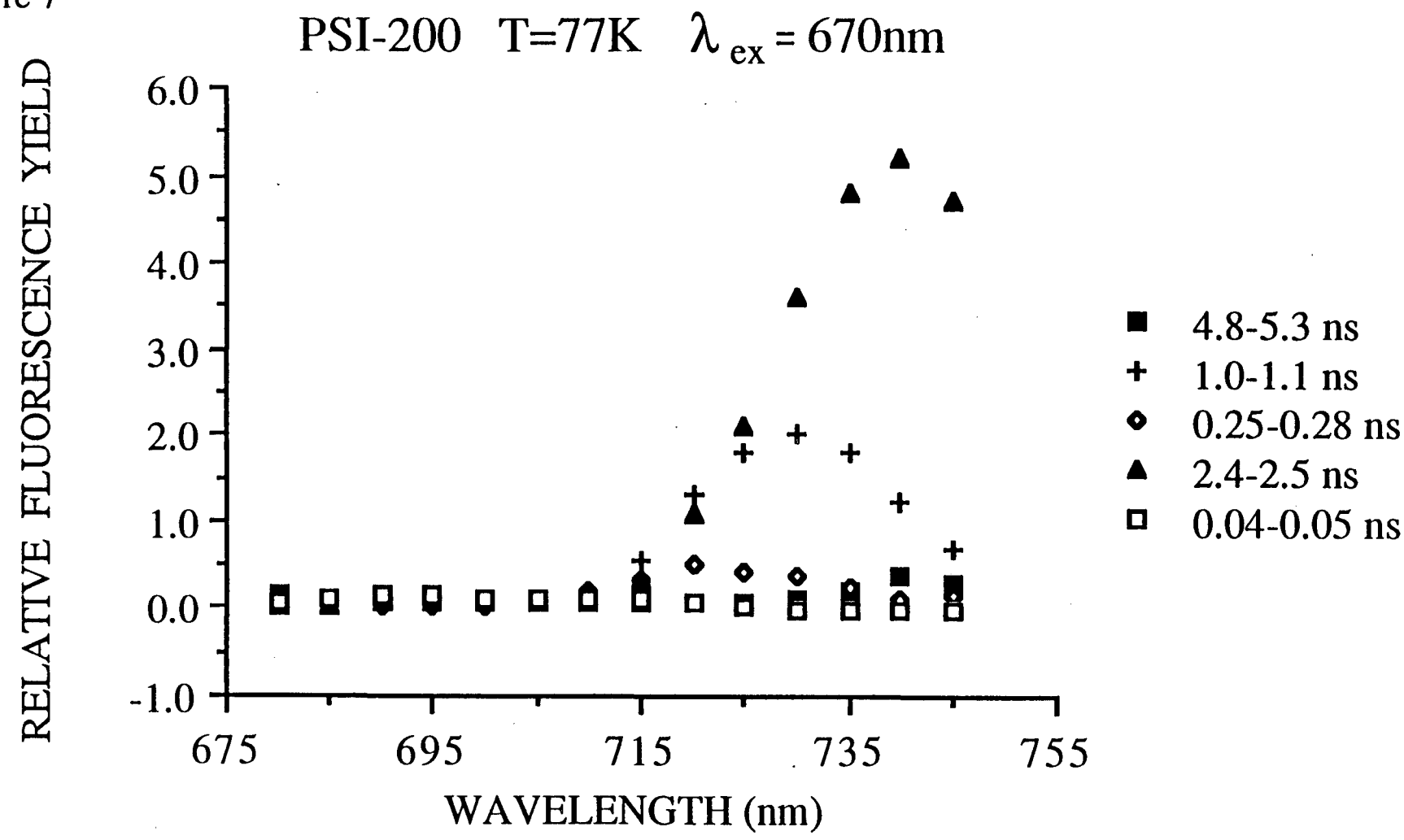
PSI-200 T=77K λ ex = 670nm
RELATIVE FLUORESCENCE YIELD
6.0
5.0
4.0
3.0
2.0
1.0
0.0
-1.0
675
695
715
735
755
WAVELENGTH (nm)
4.8-5.3 ns
1.0-1.1 ns
0.25-0.28 ns
2.4-2.5 ns
0.04-0.05 ns

Figure 8

Model of Antenna Organization in PSI-200

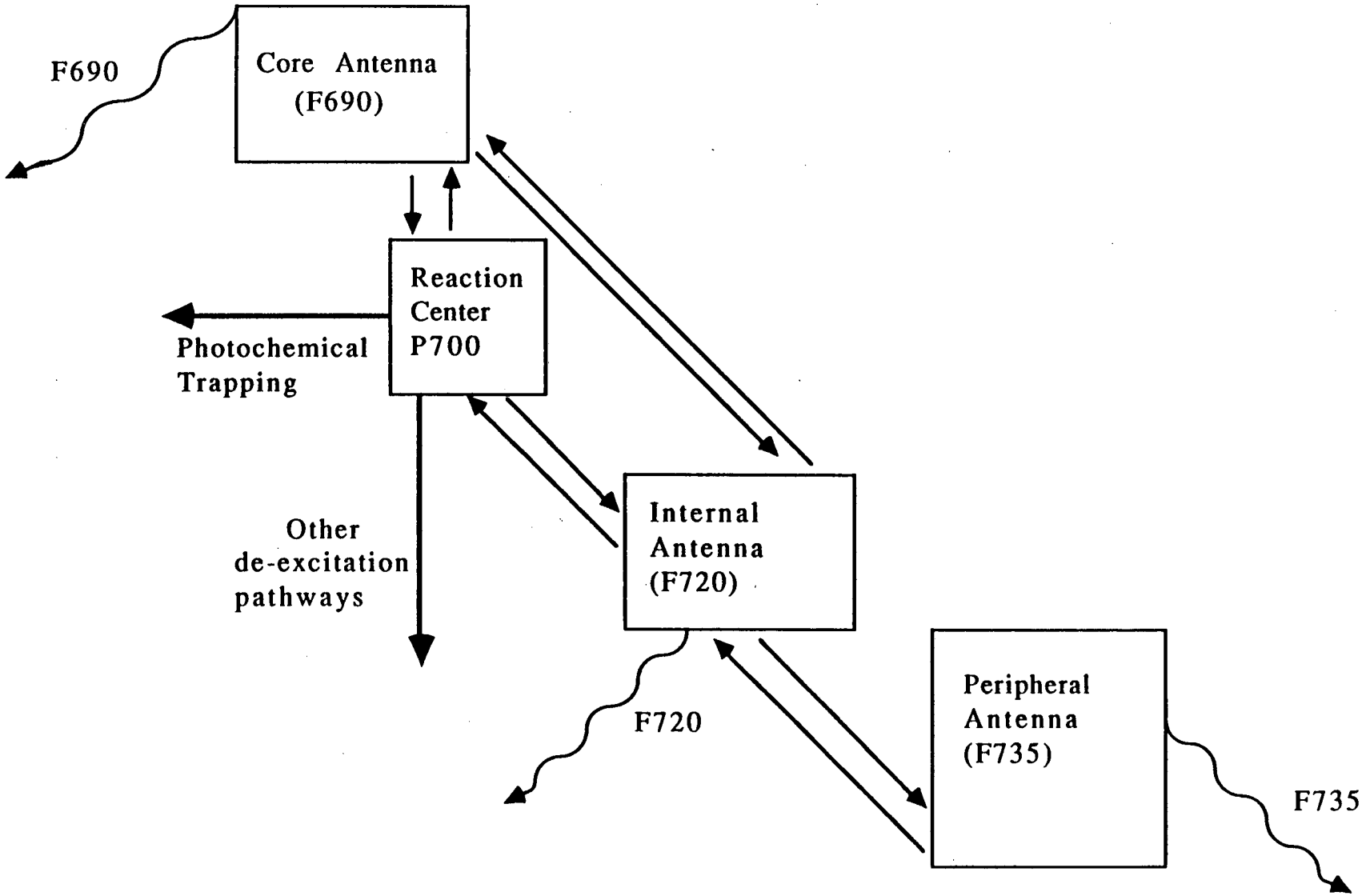

LAWRENCE BERKELEY LABORATORY
TECHNICAL INFORMATION DEPARTMENT
UNIVERSITY OF CALIFORNIA
BERKELEY, CALIFORNIA 94720